HT analysis of environmental conditions affecting expression of *tdaCDE* in *Phaeobacter* spp.

Special project 15 ECTS, carried out in autumn 2022 at DTU Bioengineering

Authors: Robert Friis-Møller, Frederik Reimert

Supervisors: Shengda Zhang, Lone Gram

DTU Bioengineering
Institut for Bioteknologi og Biomedicin

Søltofts Plads
Bygning 221
2800 Kongens Lyngby

Tlf. 50 51 26 00
20 11 88 65

www.dtu.dk

Abstract

With the world population expected to reach approx. 10 billion people by 2050 and an increasing proportion of global fish stocks classified as overfished, aquaculture is gaining significance as a source of high-quality food protein. However, intensive fish-rearing operations are prone to outbreaks of bacterial diseases caused by pathogens such as *Vibrio*, *Aeromonas* and *Tenacibaculum* spp., potentially causing fish larval populations to collapse. Several members of the marine *Roseobacter* group, such as *Phaeobacter piscinae*, produce the antimicrobial molecule tropodithietic acid (TDA), which has antagonistic properties towards several fish pathogens, including *Vibrio* spp. Given that TDA is the compound mediating the anti-pathogen effect, understanding under which conditions the molecule is produced is important. Attempts to detect the compound in algal and other natural systems by chemical analyses have been unsuccessful, and in this study we used gene expression analyses as a proxy. The purpose of this study was to determine the effect of environmental factors on the expression of the TDA-associated *tdaCDE* operon by fluorescence measurements of the reporter strain *P. piscinae* pBBRMCS1-PtdaC-GFP. In contrast to earlier studies, where biologically active TDA has been detected in substrate with high iron concentrations, the highest *tdaCDE* transcription levels and TDA concentrations were observed in growth media with a low iron concentration.

Study importance

This project supports United Nations (UN) Sustainability Goals #2 (Zero hunger), #12 (Responsible consumption & production), #13 (Climate action) and #14 (Life under water). By generating knowledge about probiotic *Roseobacter* strains and their bioactive secondary metabolites, this project contributes to the development of sustainable biocontrol solutions in the aquatic food production chain. Addition of probiotic, tropodithietic acid (TDA) producing *Phaeobacter* spp. is a potentially safe alternative to traditional antibiotic treatments in larvi- and aquacultures.

Introduction

At the time of writing, the Earth is home to approximately 8 billion people, and according to the United Nations (UN) Population Division, this number could reach between 9.4 and 10 billion by 2050 [1]. Supplying a growing population with food, including high quality protein poses a major challenge for the global food system. According to the Food and Agriculture Organization of the United States (FAO), about 3.1 billion people worldwide rely on fish for 20% of their protein intake, yet a large and increasing proportion of marine fish stocks are overfished [2]. The farming of fish (and other aquatic animals and plants), so-called aquaculture, can reduce the strain of large-scale fishing operations on marine ecosystems. In 2020, aquaculture (excluding algae production) made up approx. 50% of the global fishery production compared to 25% in 2000.

Aquaculture, like all intensive animal rearing operations, are prone to rapid disease outbreaks, which regularly cause populations of both premature and adult fish to collapse [3]. In order to reduce infections in larval rearing facilities from pathogens such as *Vibrio, Aeromonas* and *Tenacibaculum* spp., large quantities of antibiotics have been used [3]. Uncontrolled use of antibiotics contributes to the spread of antimicrobial resistant (AMR) pathogens, which may cause as many as 10 million deaths annually by 2050 [25].

Several strategies can be pursued to ensure disease control without antibiotics. Vaccines have, in some cases, been instrumental in causing rapid and dramatic reductions in the use of antibiotics. A good example is the Norwegian salmon industry, which has managed to reduce the antibacterial veterinary medical products used in aquacultures by 99.9% from 1987 to 2021 [30]. However, vaccines are not always a viable option, for instance, the fish larval immune system is not sufficiently developed to rely on vaccines for disease control [29]. To prevent a collapse in larval populations while reducing conventional antibiotic use, addition of probiotic organisms capable of antagonizing larval pathogens may prove a viable strategy [4]. Some of the most promising organisms for probiotic use in marine aquaculture belong to the *Phaeobacter* genera of the marine *Roseobacter* group [5,6]. This diverse group of α-proteobacteria inhabit the surface of coastal water, harbours, and aquaculture units worldwide, averaging 3.8% of bacterial populations [7]. Members of this group, such as *Phaeobacter piscinae* and *Phaeobacter inhibens*, are capable of antagonizing *Vibrio* and *Aeromonas* spp. *In situ* while having minimal effect on the native larval microbiota [5,6]. *Phaeobacter* spp. have been isolated from aquaculture units in Spain, Denmark and Greece [24], making them suitable for growth in larval rearing and algal feedstock cultivation facilities. Antagonism to *Vibrio* spp. has been correlated with the production of tropodithietic acid (TDA), a secondary metabolite with antimicrobial activity and cation

chelating properties [8,9]. Some studies have also found the TDA may be involved in quorum sensing signalling and the production may itself be under QS control [18].

The antimicrobial mechanism of action (MoA) of TDA is based on an antiporter mechanism [9] (Figure 1). In its acid form, TDA is capable of diffusing across the cell membrane. In the cytosol, the carboxylic acid group is deprotonated, decreasing the pH of the cytosol.

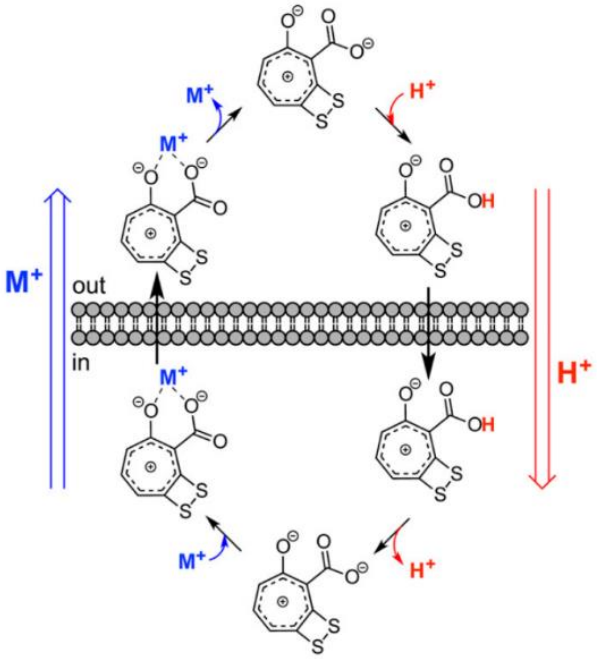

Figure 1: The antimicrobial MoA of TDA. The cytosolic pH of the target cell is lowered while cations, such as Fe^{3+}, are exported. [9]

TDA is capable of chelating biologically important cations such as Fe^{3+}/Fe^{2+}, Zn^{2+} and Mn^{2+} (collectively M^{+}). The TDA-M^{+} complex can then diffuse out of the cell in clusters, destabilizing the cell membrane. The iron-chelating properties of TDA may have evolved to scavenge cations in marine environments, in which metals such as iron, zinc and manganese are limiting factors for growth. [31]

Earlier research into probiotic *Roseobacter* strains quantified TDA production by measuring the brown "pigmentation" caused by the TDA chelation of iron, or the zone of inhibition caused by filtered supernatant when added to cultures of *Vibrio* or *Aeromonas* spp. [10,11]. The brown pigmentation is a [TDA-Fe^{3+}] complex, which is an indicator of TDA presence in iron rich environments [27]. However, using it as a sole proxy of TDA production can be misleading. The pigmentation caused by the [TDA-Fe^{3+}] complex does not necessarily correlate with the concentration of TDA in the media. Furthermore,

the presence of brown pigmentation from the [TDA-Fe^{3+}] complex can be difficult to differentiate from free iron complexes, colony- and biofilm formation, among other factors.

The use of inhibition assays as a method of TDA quantification assumes that TDA exists as a single, antimicrobial structure. However, some studies have proposed the existence of a non-antimicrobial form of TDA, sometimes referred to as 'pre-TDA', produced under iron-limited conditions [11,26]. Furthermore, the entirety of the TDA biosynthesis has yet to be established [12]. Thus, an improved and preferably real-time method of TDA quantification is necessary to determine the influence of environmental factors on the production of TDA and the transcriptional regulation of the TDA-associated biosynthetic gene cluster (BGC).

Scope & aim of experiments

The aim of this project was to analyse how environmental factors affected transcription of the *tdaCDE* region of the TDA-associated BGC. This was used as a proxy to chemical detection of TDA. To achieve this, a green fluorescent protein (GFP) reporter strain of *Phaeobacter piscinae* S26 [5], constructed by Shengda Zhang (ORCID No. 0000-0002-2220-3904) and Jette Melchiorsen (SCOPUS ID: 6506710191) was used to quantify transcription by fluorescence measurements. The strain *P. piscinae* S26 (16S-rRNA GenBank no. AJ536670.1) was chosen for its high production of brown pigment when grown in marine broth (MB) [5]. This has previously been interpreted as an indicator of TDA production [27]. *P. piscinae* S26 was originally isolated from a Greek aquaculture unit and characterized by Sonnenschein et al. in 2016 [24].

In our experiments, we aimed at studying the effect of media composition, CasAmino acids (CasA) concentration, presence of 0.5 mM Fe^{3+} and N-source on transcription of *tdaCDE* genes. To determine actual presence of TDA *in vitro*, a chemical extraction and liquid chromatography mass spectrometry (LC-MS) analysis for secondary metabolites was conducted in cooperation with Michael Scott Cowled (ORCID No. 0000-0002-5083-3532) of the Natural Product Discovery group at DTU Bioengineering.

Materials & methods

Description of strains

The following bacterial strains were used in this study (Table 1):

Table 1: Description of strains used in this study.

Strain name	Description
Phaeobacter piscinae S26 (JSWK01) WT	Isolated from a Greek aquaculture system and characterized by Grotkjær et al. in 2016 [5]. GenBank no. AJ536670.1. Encodes kanamycin resistance marker (*kanR*).
Phaeobacter piscinae S26 + pBBRMCS2-PtdaC-GFP (S26-GFP)	Reporter fusion constructed by Shengda Zhang and Jette Melchiorsen. Holds the pBBRMCS2-PtdaC-GFP plasmid w. *gfp* gene fused to the P*tdaC* promoter. Encodes kanamycin resistance marker (*kanR*).
Phaeobacter piscinae S26 + pBBR-MCS2 (empty vector, S26-NC)	Holds the promoterless pBBR-MCS2 plasmid. Negative control strain. Encodes kanamycin resistance marker (*kanR*).

Media and growth conditions

For the cultivation experiments, the following media types and stocks were used: 3% (w/v) Instant Ocean (IO: Instant Ocean® Sea Salt, No. SS15-10) was used as a base for supplementation with different carbon- and nitrogen sources. ½ Yeast Tryptone Sea Salt (1/2 YTSS: 0.2% of Yeast Extract, 0.125% Tryptone, 2% Sigma Sea Salts) [32] and Difco Marine Broth 2216 (MB, BD Difco Cas No. 10043-52-4) were used as complex growth media. Physiology, TDA production and growth kinetics of *Phaeobacter* spp. have previously been studied using these media types.
F/2 Media [33] was used as a defined minimal growth medium.

CasAmino acids stock (Thermo-Fischer Scientific, catalog no. 223050) was prepared in 30% w/v solution, filtered through a 0.22 µm filter (Sartorius Minisart® Syringe Filter, Item no. 16532) and transferred to 2 mL aliquots. Aliquots were stored at -20°C.
CasAmino acids were added to growth media a final concentration of 0.3% w/v. In all IO-based media types, CasAmino acids functioned as the sole nitrogen source.

Glucose stock (Sigma-Aldrich, Cas no. 50-99-7), was prepared in 20% w/v solution, filtered through a 0.22 µm filter (Sartorius Minisart® Syringe Filter, Item no. 16532) and transferred to a sterile 50 mL blue cap bottle. Glucose was added to growth media to a concentration of 0.2% w/v. Stock was stored

at room temperature, approximately 20°C. Glucose was used as a supplementary carbon source in IO + CasA media, and as the sole carbon source in F/2 based media.

For media supplemented with ferric iron, $FeCl_3$ stock (Sigma-Aldrich, Cas No. 7705-08-0) was prepared in 0.5 M solution (filtered through a 0.22 µm filter (Sartorius Minisart® Syringe Filter, Item no. 16532)). and added to a final concentration of 0.5 mM (1000x dilution). $FeCl_3$ was chosen for its superior solubility compared to ferric citrate, $C_6H_5FeO_7$. [11]. The final iron concentration of 0.5 mM is similar to MB and is comparable to previous studies. Stock was stored at room temperature, approximately 20°C, and covered in tin foil to block light.

NH_4Cl stock (Sigma-Aldrich, Cas No. 12125-02-9) was prepared in 0.5 M solution (filtered through a 0.22 µm filter Sartorius Minisart® Syringe Filter, Item no. 16532)) and added to a final concentration of 1.0 mM. NH_4Cl is typically used as a nitrogen source addition to F/2 media in cultivation of microalgae. For future studies into algae/bacteria interactions, we wanted to assess the growth and *tdaCDE* transcription levels of *P. piscinae* in this media composition.

Kanamycin sulfate stock (Sigma-Aldrich Cas No. 25389-94-0) was prepared to a concentration of 100 mg/mL and added to the media to a final concentration of 200 µg/mL. For the last experiments exploring the effect of varying nitrogen sources on *tdaCDE* transcription, a kanamycin concentration of 100 µg/mL was used.

Marine agar (MB w. 15 g agar/L) with kanamycin was used to culture bacterial strains from cryostocks at -80°C. Strains were inoculated in MB+Kan media, and precultures were grown w. shaking for 24-48 hours at 25°C. The final cell concentration of precultures was estimated to ~10^8 CFU/mL by colony counting. For each cultivation, the concentration of cells at inoculation was ~10^4 CFU/mL.
Pre-cultures of *P. piscinae* S26 grown in MB displayed dark pigmentation after approx. 24h of growth. Cultures grown in iron-deficient media had only slight pigmentation, likely resulting from cells in suspension.

To assess transcription of *tdaCDE* in *P. piscinae* S26-GFP in different media types, OD600 and relative GFP fluorescence were measured through high-throughput cultivation in 96-well microwell plates in an Agilent Cytation 5 Cell Imaging Multimode Reader using Nunc™ MicroWell™ 96-Well microplates (Thermo-Fischer Scientific, catalogue no. 243656). Inoculation of microplates was performed by mixing of media and culture in a deep well plate to specified concentrations, whereafter 200 µL of

mixture was transferred to the corresponding position of the microplate.
Plates were incubated at 25°C with continuous shaking for 72-96 h. OD600 and GFP signal measurements were taken every 20 minutes. Wavelength of emission and excitation?

Chemical detection of TDA in IO +/- Fe^{3+} and MB

To determine a correlation (or co-occurrence of) between transcription of *tdaCDE* and presence of TDA, chemical extraction and LC-MS detection of TDA was performed. From cultures of *P. piscinae* S26-GFP and *P. piscinae* S26-PNC in IO+Glc (0.2% w/v)+CasAmino acids (0.3% w/v) +/ -Fe^{3+} (0.5 mM) + Kan (100 µg/mL) and MB+Kan (200 µg/mL), secondary metabolites were extracted by addition of ethyl acetate (EtOAc, Sigma-Aldrich, Cas No. 141-78-6) with 1% formic acid (FA, Sigma-Aldrich, Cas No. 64-16-6), followed by organic phase separation and evaporation under N_2 blowdown. Remaining dry mass was resuspended in methanol (MeOH, Sigma-Aldrich Cas no. 67-56-1). LC-MS detection of TDA was performed by Michael Scott Cowled of the Natural Product Discovery group at DTU Bioengineering.

Analysis of N-source dependency of *tdaCDE* transcription

To determine how *tdaCDE* transcription depends on nitrogen sources, two assays were performed with BioLog PM3B Phenotypic Screening microwell plates. A preculture of *P. piscinae* S26-GFP was inoculated into IO+Glc (0.2% w/v)+Kan (100 µg/mL) to a concentration of ~10^4 CFU/mL. This suspension was added to each well of a BioLog PM3B 96-well microplate and pipetted up and down to dissolve nitrogen source. 100 µL was then taken from each well and added to the corresponding position in a Nunc™ MicroWell™ 96-Well microplate. Cultivation and measurement of growth (OD) and gene transcription (fluorescence) was performed using the same protocol as previous cultivation experiments.

Data analysis

The data handling was all done in the statistical computing software R (R Core Team (2022). https://www.R-project.org/.) using the dplyr package (dplyr: A Grammar of Data Manipulation. https://github.com/tidyverse/dplyr). Optical density at 600 nm (OD) and relative fluorescence units (RFU) datapoints from each microplate well were adjusted to the background readings from the media, by subtracting the media negative control reads as follows:

$$Adjusted(x) = Value(x) - Value(x)$$

Relative fluorescence was calculated using the following formula:

$$Relative(RFU) = \frac{Adjusted(RFU)}{Adjusted(OD)}$$

This was only done for OD and RFU reads above 0 were to avoid magnification of negative value outliers. The OD and relative RFU values were plotted using the ggplot2 package (ggplot2: Elegant Graphics for Data Analysis, https://ggplot2.tidyverse.org). The OD vs time graphs are plotted using locally estimated scatterplot smoothing (LOESS), with a very minor smoothing span=0.2. This is done in order to visualize the growth phases more defined along with a rolling standard deviation. To calculate growth parameters, datapoints from selected wells were cropped around the exponential phase. Then they were modelled to fit a logistic regression using GrowthCurver [28] with the following form:

$$N_t = \frac{K}{1 + \left(\frac{K - N_0}{N_0}\right) e^{-rt}}$$

Where N denotes the population measured in OD at a certain timepoint, the rate of growth ® determines how quickly the population grows, the carrying capacity (*K*) determines the maximum size that the population can reach, and time (*t*) represents the passage of time. The raw data long with the R script used for the data analysis in this article can be found in the supplementary material.

Results

Assessment of reporter strain GFP signal compared to WT and NC

To determine if the reporter strain *P. piscinae* S26-GFP produced a measurable fluorescence signal compared to autofluorescence of a wild-type (WT) strain, cultures were compared under inverted epifluorescence microscopy (Nikon Inverted Fluorescence Microscope Eclipse TI2) at 60x magnification. By qualitative assessment, it was determined that the reporter strain produced a measurable GFP-signal compared to the WT (Figure 2).

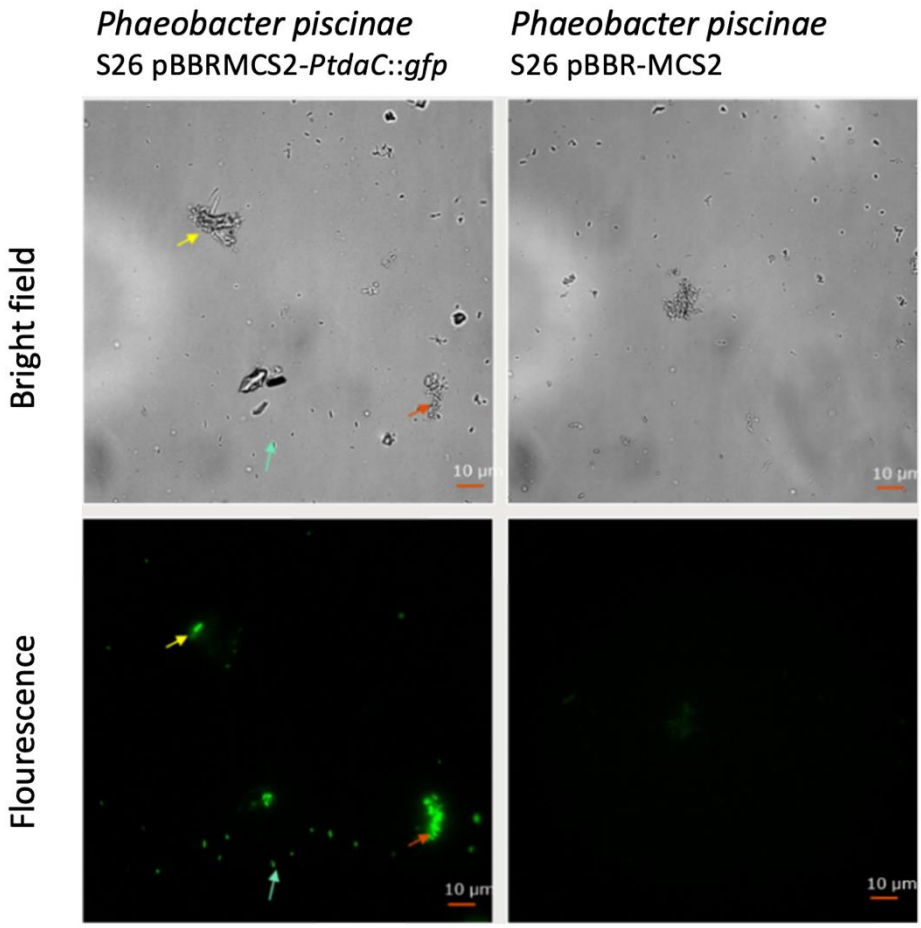

Figure 2: Inverted epifluorescence & bright field microscopy imaging of *P. piscinae* S26-GFP compared to a WT *P. piscinae* S26. Red arrow indicates GFP-signal in a colony aggregate. Green arrow indicates fluorescence in single cells. Imaging by Shengda Zhang and Jette Melchiorsen.

To quantify the GFP signal of the reporter strain compared to the NC strain, fluorescence measurements of both strains were compared to a media NC (only media) sample. The difference in OD600 readings between the GFP Strain (OD 90.1±14.3) and NC Strain (OD 95.8±4.2) were NS (non-significant), but a statistically significant difference in accumulated GFP signal between them was established (Welch's t-test, p = 0.0049). (Figure 3)

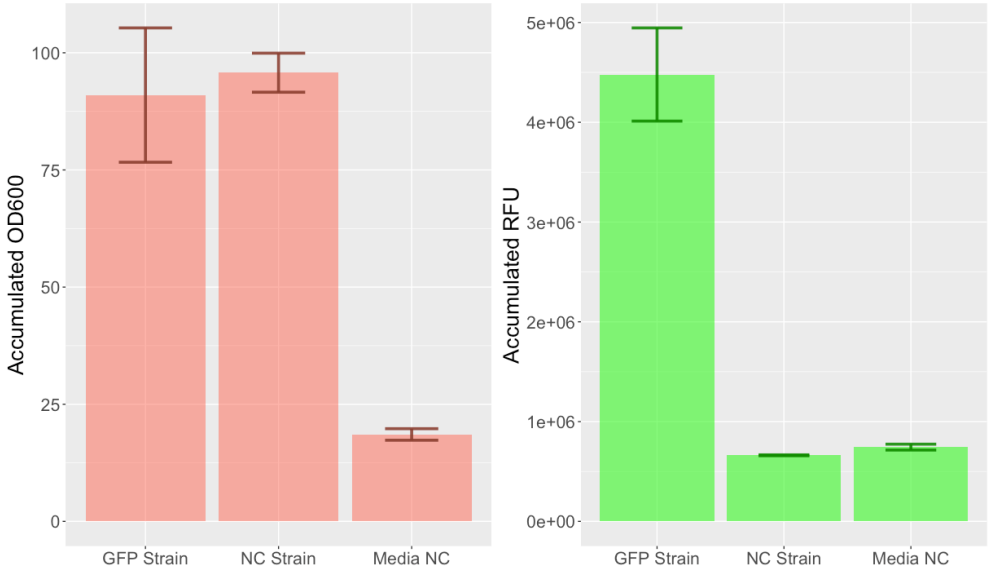

Figure 3: The average accumulated OD and RFU reads along with the standard deviation calculated from each of the three *P. piscinae* S26-GFP, *P. piscinae* S26-NC and Media NC replicates grown on 1/2YTSS media for 96 hours in a Nunc™ MicroWell™ plate. (n=3)

Effect of media composition on *tdaCDE* transcription

To analyze the effect of different types of media on *tdaCDE* transcription, high-throughout 96-well microplate cultivation experiments were performed. The highest GFP signal relative to OD600 was observed in IO media containing CasAmino acids as the sole C- and N-source (Figure 4). No growth was observed in IO media containing only glucose.

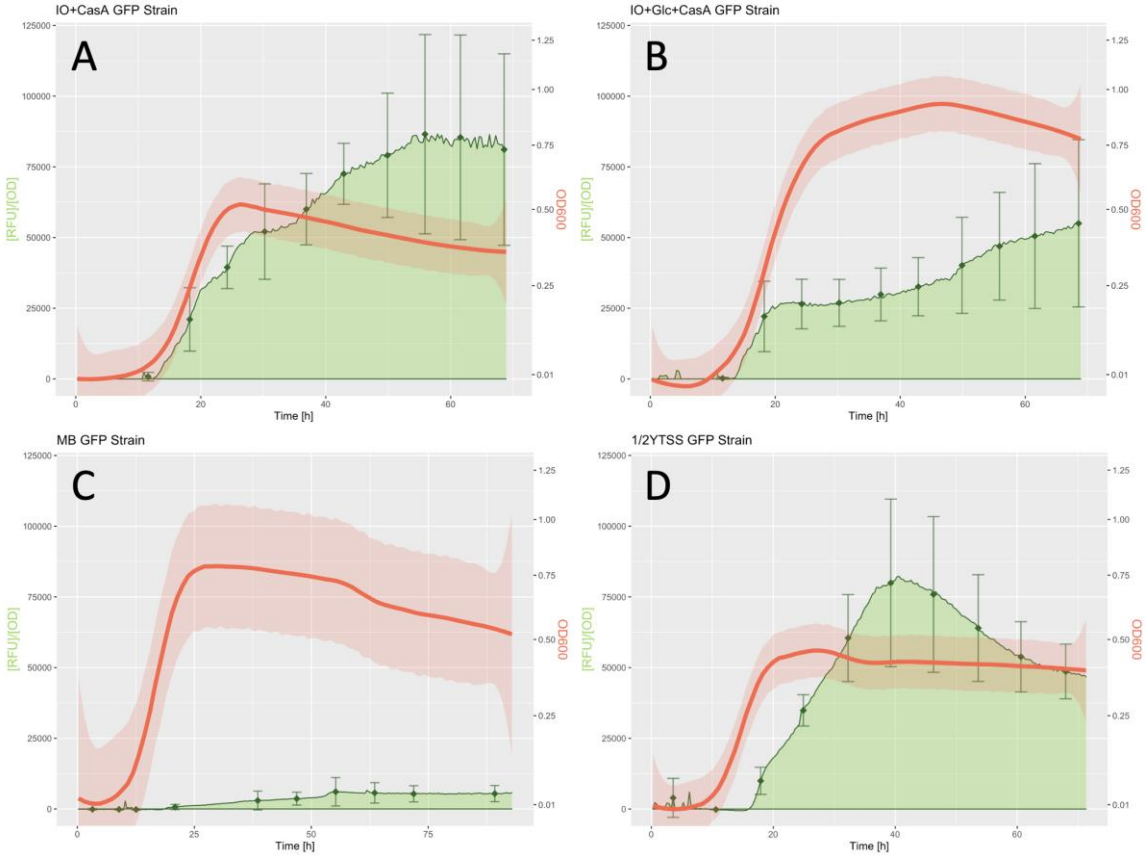

Figure 4: OD600 and relative GFP-signal measured in RFU/OD over time (*t*, [h]) for *P. piscinae* S26-GFP in **(A)** IO+CasA, **(B)** IO+Glc+CasA, **(C)** MB and **(D)** 1/2YTSS. Data was generated from three biological replicates. Error bars and transparent fill indicate standard deviation. Red line represents OD measurements over time (*t*) on a log10-scale axis. Green line w. fill represents GFP-signal normalized to OD measurements [RFU/OD] over time (*t*). (n=3)

Compared with IO+CasA media (Figure 4A), cell growth was significantly improved by addition of 0.2% w/v glucose (Figure 4B, Welch's t-test on accumulated OD600, p = 0.0481). Accounting for time delays between transcription initiation/termination and translation, *tdaCDE* transcription was initiated in early exponential phase. In IO-based media, a second induction of *tdaCDE* transcription was observed in early stationary phase, which lead to a further increase in GFP signal to a sustained maximum. This second induction appeared independently of lag- and exponential phase duration. A significantly higher GFP signal was measured in IO-based media compared to MB (Welch's t-test, p = 0.0205). No significant differences in GFP signals were observed between IO media types and 1/2YTSS, but a GFP signal reduction during the stationary phase was observed in 1/2YTSS.
It was concluded that the media generating the highest GFP signal, and by proxy *tdaCDE* transcriptional activity, was IO+CasA media.

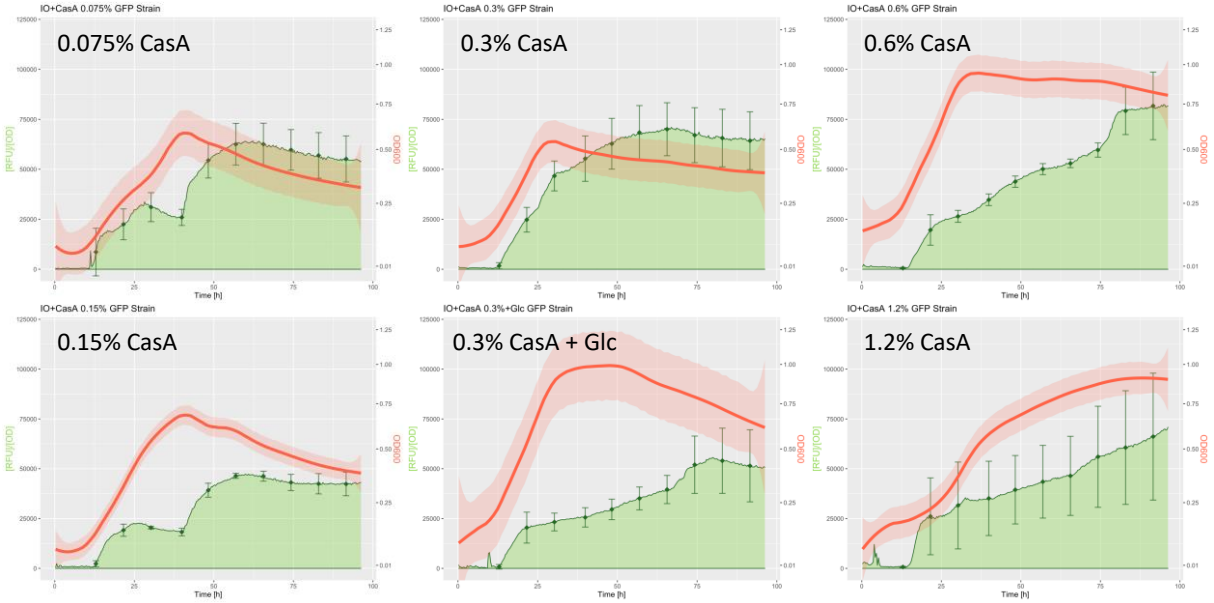

Figure 5: OD600 and relative GFP-signal measured in RFU/OD over time (*t*, [h]) for *P. piscinae* S26-GFP in CasAmino acid concentrations 0.075%, 0.15%, 0.3%, 0.6% and 1.2%. Red line represents OD measurements over time (*t* [h]) on a log10-scale axis. Green line w. fill represents GFP-signal normalized to OD measurements [RFU/OD] over time (*t* [h]). (n=3)

As CasA containing media produced the highest GFP signal, the effect of CasA concentration on *tdaCDE* transcription was studied in a similar experimental setup (Figure 5).

Cell levels reached a maximum at 0.3% CasA w. glucose and 0.6% CasA w/o glucose. An increase in relative GFP-signal was observed at CasA concentrations at >0.3% w/v compared to =0.3%. A doubling of CasAmino acid concentration from 0.3% w/v to 0.6% w/v led to a proportional doubling of maximum GFP-signal, but this effect was transient. At a concentration of 1.2% w/v, the growth rate of cells was reduced, and the signal pattern could not be confirmed within the timeframe of the experiment. No significant change in relative GFP-signal was observed. This suggests that increasing concentrations of CasAmino acids (interval 0.015-1.2%.) have a diminishing effect on the relative transcription of *tdaCDE*.

Effect of nitrogen sources on *tdaCDE* transcription

As CasAmino acids are a complex blend of amino acids, it is difficult to determine whether an individual nitrogen source produces an observed increase in *tdaCDE* transcription. Therefore, the influence of individual nitrogen sources on *tdaCDE* transcription was analyzed by microplate cultivations on N-

sources extracted from a BioLog Phenotypic Microarray (BioLog PM3B MicroPlate™). N-sources were ranked by the mean sum of absolute GFP-signal over the entire cultivation period (Figure 6):

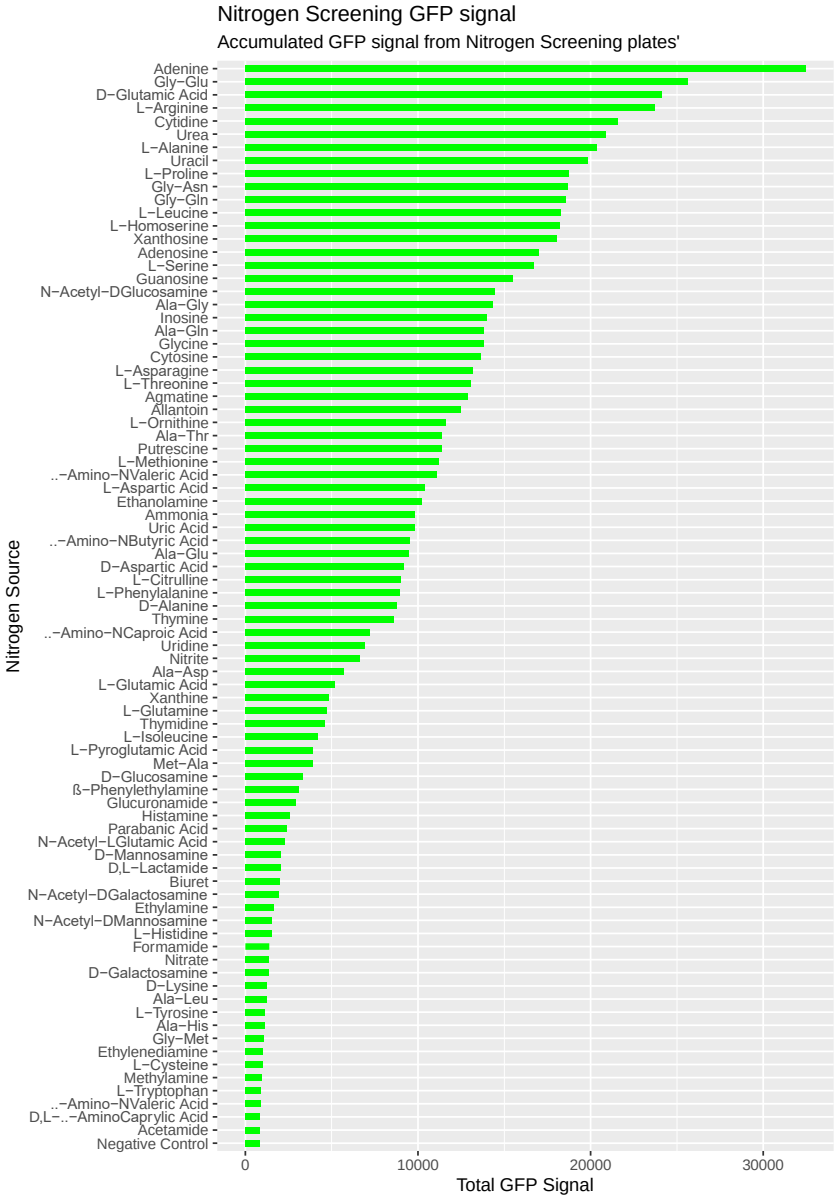

Figure 6: The top 20 RFU signals measured by the mean sum (n=2) of GFP signals as well as OD in cultivation of *P. piscinae* S26-GFP on nitrogen sources extracted from a BioLog PM3B MicroPlate™. The rest of the dataset can be seen in Appendix 1.

A large variability in total GFP-signal was observed across N-sources (Figure 6). Extrapolating from this and previous experiments, it was concluded that varying N-source compositions in growth media influences *tdaCDE* transcription. 9 out of the top 20 GFP response N-Sources (Figure 6) contain cyclical structures, which are suggested to act as precursors for bacterial tropone biosynthesis [12,20].

Effect of Fe^{3+} on *tdaCDE* transcription and presence of TDA *in vitro*

It has previously been shown that production of bioactive TDA *in vitro* is linked to the presence of iron in the growth medium [11,27]. The effect of Fe^{3+} on *tdaCDE* transcription was tested in our experiments (Figure 7).

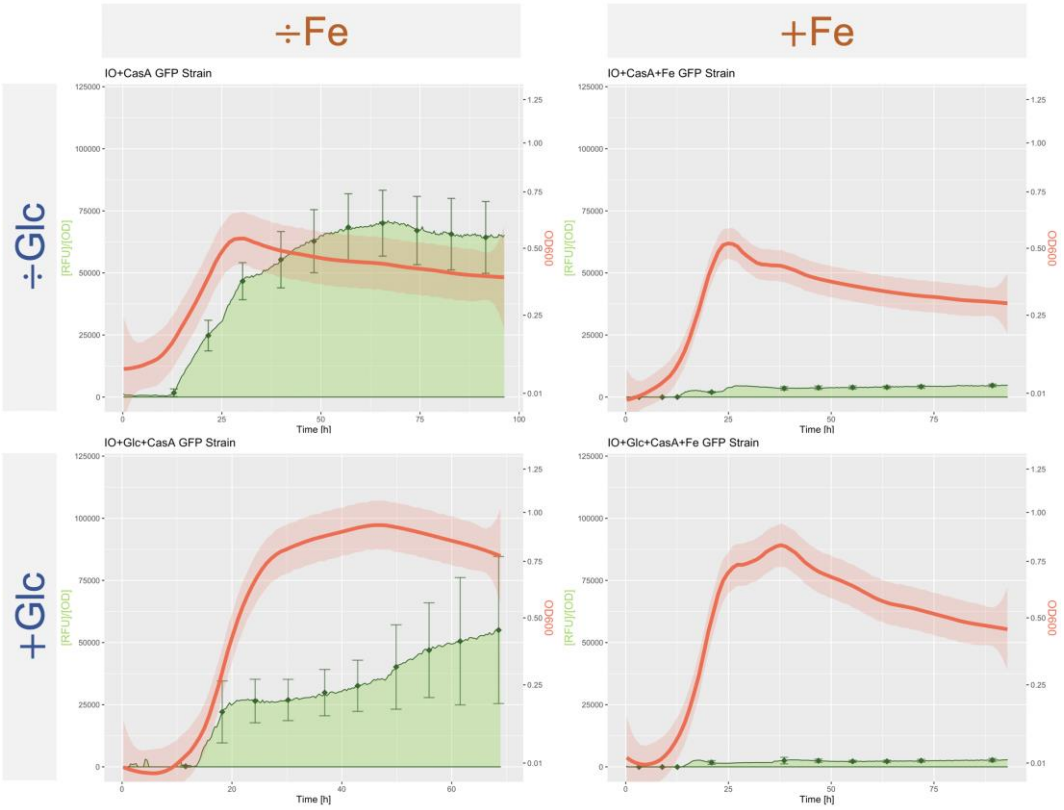

Figure 7: Effect of Fe^{3+} on *tdaCDE* transcription in *P. piscinae* S26-GFP cultivated in IO+CasA growth media. Addition of Fe^{3+} significantly reduced the measured GFP-signal and shortened generation time [h].
(CasA=0.3%, Glc=0.2%, [Fe^{3+}]=0.5 mM). Red line represents OD measurements over time (*t*) on a log10-scale axis. Green line w. fill represents GFP-signal normalized to OD measurements [RFU/OD] over time (*t*). (n=3)

In both IO+CasA and IO+CasA+Glc media, a significantly lower average relative GFP-signal was observed in the presence of Fe^{3+} as compared to iron deficient media (Welch's t-test, p = 0.00232 and 0.0329 respectively), (Figure 7). When glucose was added to the cultures (+/¸ Fe), the carrying capacit increased significantly (Welch's t-test, p = 0.00379 and 0.0339 respectively). A significant decrease in

generation time [h] was observed when Fe^{3+} was added to the -Glc culture but not in the +Glc culture (Welch's t-test, p = 0.00324 and 0.0915). The growth curves were modelled to logistic regression to estimate the growth parameters (Appendix 2, Table 2).

Table 2: Parameter data and standard deviation for *P. piscinae* S26-GFP in IO+CasA media with and without Fe^{3+} and Glc. Data derived from models seen in Appendix 2. (n=3)

	Mean GFP [RFU]	Carrying Capacity K [OD]	Generation time r [h]
IO + CasA	48202 ± 9319	0.441 ± 0.109	2.267 ± 0.211
IO + CasA + Fe	3307 ± 481	0.541 ± 0.094	1.707 ± 0.241
IO + CasA + Glc	49755 ± 15459	0.961 ± 0.121	2.604 ± 0.258
IO + CasA + Glc + Fe	1909 ± 494	0.806 ± 0.109	2.06 ± 0.325

To link transcription patterns to the actual presence of TDA in the growth media, a chemical extraction and LC-MS analysis was performed. The relative intensity (RI) of the m/z-signal of TDA normalized to carrying capacity in OD600 was measured for cultivations in MB and IO+CasA+Glc(+/-)Fe^{3+} (Figure 8).

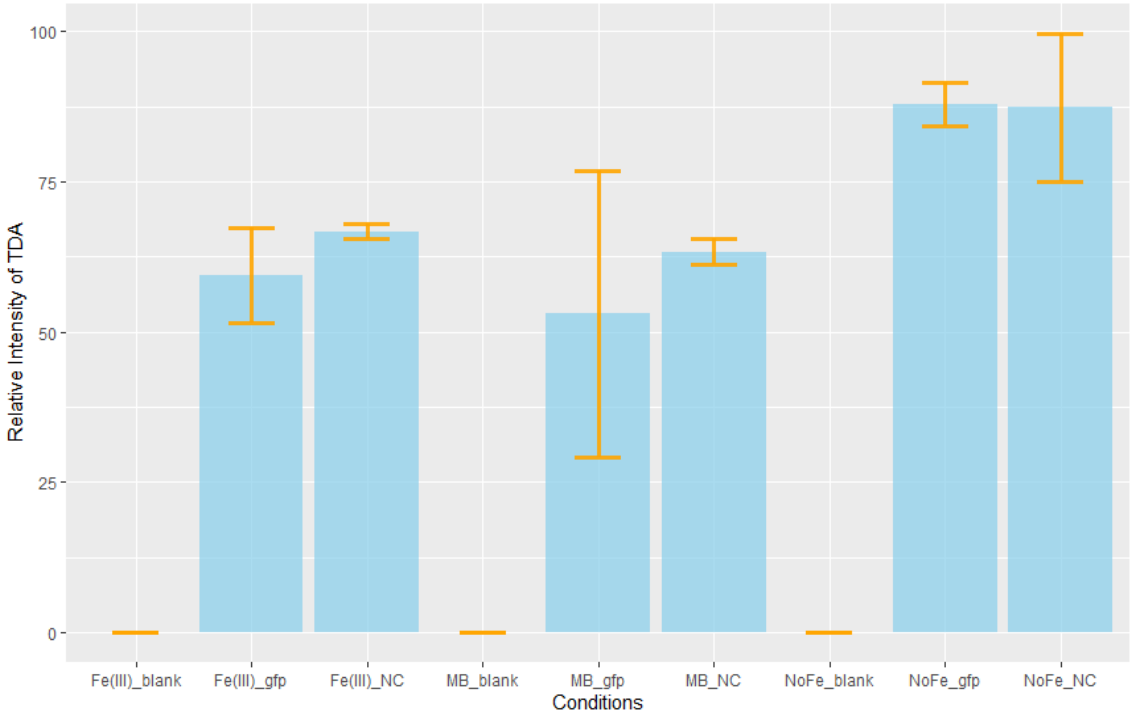

Figure 8: Relative intensity of m/z signal from LC-MS analysis of media from *P. piscinae* S26-GFP cultivation in IO+CasA+Glc(+/-)Fe^{3+} and MB. Blanks indicate media NC. Error bars indicate standard deviations (n = 3).

Based on overlap of standard deviations, a significantly higher amount of TDA was present in media without Fe^{3+} on a significance threshold of 5%. Noticeably, the difference in TDA content in IO (+/÷) Fe^{3+} media is not proportional to the difference observed in *tdaCDE* transcription. No significant difference in results between IO+Fe^{3+} media and MB was observed. The effects of Fe^{3+} and Glc on *tdaCDE* transcription and TDA content in growth media based on our results are summarized in Table 3.

Table 3: Effect of Fe^{3+} and Glc in IO+CasA media on Mean GFP [RFU], carrying capacity *K* [OD] and generation time *r* [h]. Arrows indicate a significant increase or decrease ($p < 0.05$), and NS signifies non-significant results.

	TDA [RI]	Mean GFP [RFU]	Carrying Capacity K [OD]	Generation time r [h]
+Fe	↓	↓	NS	↓
+Glc	Unknown	NS	↑	NS

Discussion

The operon of interest in this article, *tdaCDE*, was chosen for its proposed function as a regulated link between the primary and secondary metabolism of *Phaeobacter* spp. in the context of TDA production [12,16,18]. Previous studies indicate that the P*tdaCDE* promoter is highly regulated, likely by mechanisms involving the LysR-type transcriptional regulator (LTTR) encoded by *tdaA*, quorom sensing [18] and the phenylalanine catabolon (PAAC, genes *paaABCE*, *paaK*, *paaZ/Z2* and *tdaF*) [12,16].
Our GFP signal measurements, and by proxy *tdaCDE* transcription levels, were obtained from an extrachromosomal element: The pBBRMCS2-PtdaC-GFP plasmid. In *Phaeobacter* spp., the native P*tdaCDE* promoter is encoded on a megaplasmid element (chromid) approx. 262-kbp in size [19]. Direct interactions between the *tdaCDE* operon and other TDA-associated genetic elements may not be reflected accurately in our results, such as the relationship with the PAAC, *tdaAB*, or *tdaF*.
In earlier studies, significant increases in TDA production were measured in both the early exponential phase and stationary phase [18]. In our cultivation experiments, a similar pattern of *tdaCDE* transcription was observed. Production of TDA has earlier been correlated to biofilm production and a sessile life stage, characterized by high levels of intracellular cyclic-di-GMP [11,17].

The fluorescence data has not been adjusted to the fact that the GFP protein has an unknown half-life, meaning it could theoretically accumulate in the cytosol after translation [15]. Accumulated GFP may produce skewed results of the real-time transcription of *tdaCDE*. Our GFP measurements were

calculated relative to OD600, meaning a higher relative GFP signal could also be caused by a decrease in biomass during stationary phase.

Previous work on the effect of Fe^{3+} on TDA production in *Phaeobacter* spp. indicates that TDA was only produced in high concentrations in the presence of Fe^{3+} [11]. Our experiments indicate the opposite: That *tdaCDE* transcription and TDA / TDA precursor production is higher under iron starvation. This challenges the notion that TDA is not classified as a traditional siderophore due to its production in high-iron environments [21,22]. It is unknown what precursor or analogous form of TDA exists in the growth media before extraction with acidic solvent (EtOAc + FA 1%). Acidification of media by addition of HCl has previously been shown to produce bioactive TDA from a “pre-TDA” analogue/pre-cursor expressed from the same biochemical pathway [11]. Whether the observed reduction of *tdaCDE* transcription in 0.5 mM Fe^{3+} conditions were caused by a regulatory mechanism or chemical interference with GFP is unknown, and a direct transcriptomic analysis (RT-qPCR + sequencing) would be necessary to confirm the expression profile.

Based on our experiments analysing the effect of varying N-sources on *tdaCDE* expression, it was concluded that expression varied between cultivations on different N-sources. Measurements of GFP signals were quite reliable, but growth curves (OD600) provided inconsistent results. Further experiments would be necessary to perform a more comprehensive analysis of the effects of different N-sources.

We speculate that an increased intracellular concentration of [Fe^{3+}-TDA] complex may cause negative feedback regulation of the TDA BGC. Similar mechanisms have been observed in several siderophore-producing species, for example *P. aeruginosa* [23].
Experiments analyzing *tdaCDE* transcription in growth on varying N-sources showed inter-sample differences. A speculative abundance of cyclical compounds in the Top 20 GFP producing compounds was observed, but no further investigation of specific compound classes or metabolic pathways were conducted.

Conclusions

The GFP reporter strain *P. piscinae* pBBRMCS2-PtdaC-GFP constructed by Shengda Zhang and Jette Melchiorsen produced a significantly higher baseline fluorescence signal compared to WT and NC strains. The strain functioned as a robust, real-time quantitative platform for HT *tdaCDE* gene

transcription assays. In investigating the effect of varying media compositions on the transcription of *tdaCDE*, it was found that IO media with 0.3% w/v CasAmino acids produced the highest GFP signal relative to biomass. Varying concentrations of CasAmino acids in growth media did not affect relative GFP signal intensity significantly in the interval 0.015 - 1.2% CasA (w/v). Analysis of *tdaCDE* transcription levels on varying N-sources revealed inter-sample variation in GFP signal intensity and minor differences in cell growth parameters.

In contrast to earlier studies, our experiments indicate that *in vitro* production of TDA and transcription of the *tdaCDE* operon are higher in low iron concentrations. Addition of Fe^{3+} to IO-based media was correlated to a significant reduction in OD-relative GFP signal and a lower concentration of TDA in growth media.

Acknowledgements

First and foremost, we would like to extend an enormous thanks to Shengda Zhang, Lone Gram and the rest of the Bacterial Ecophysiology and Biotechnology group at DTU Bioengineering. You have welcomed us with open arms into your community, given us fascinating learning experiences and treated us as equal friends and colleagues. We are beyond excited to continue our work with you in the future, both into our Bachelor project and perhaps even beyond. Lastly, our gratitude goes out to the Danish National Research foundation for funding the Center for Microbial Secondary Metabolites (CeMiSt), which has provided us with the necessary aid to realize our experiments.

Appendix

Appendix 1.

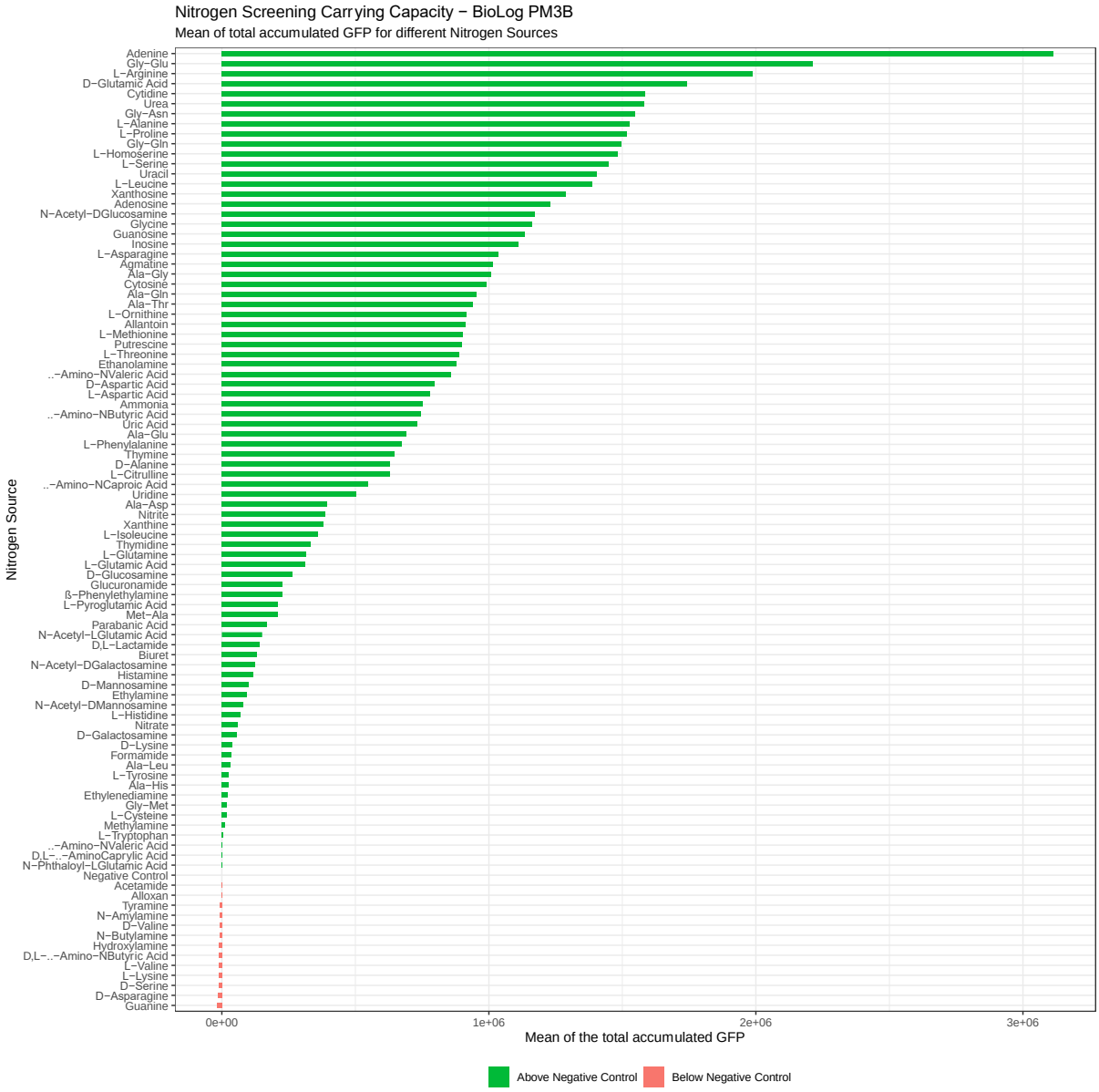

Appendix 1. RFU signals measured by the mean sum (n=2) of GFP of *P. piscinae* S26-GFP on nitrogen sources extracted from a BioLog PM3B MicroPlate™.

Appendix 2.

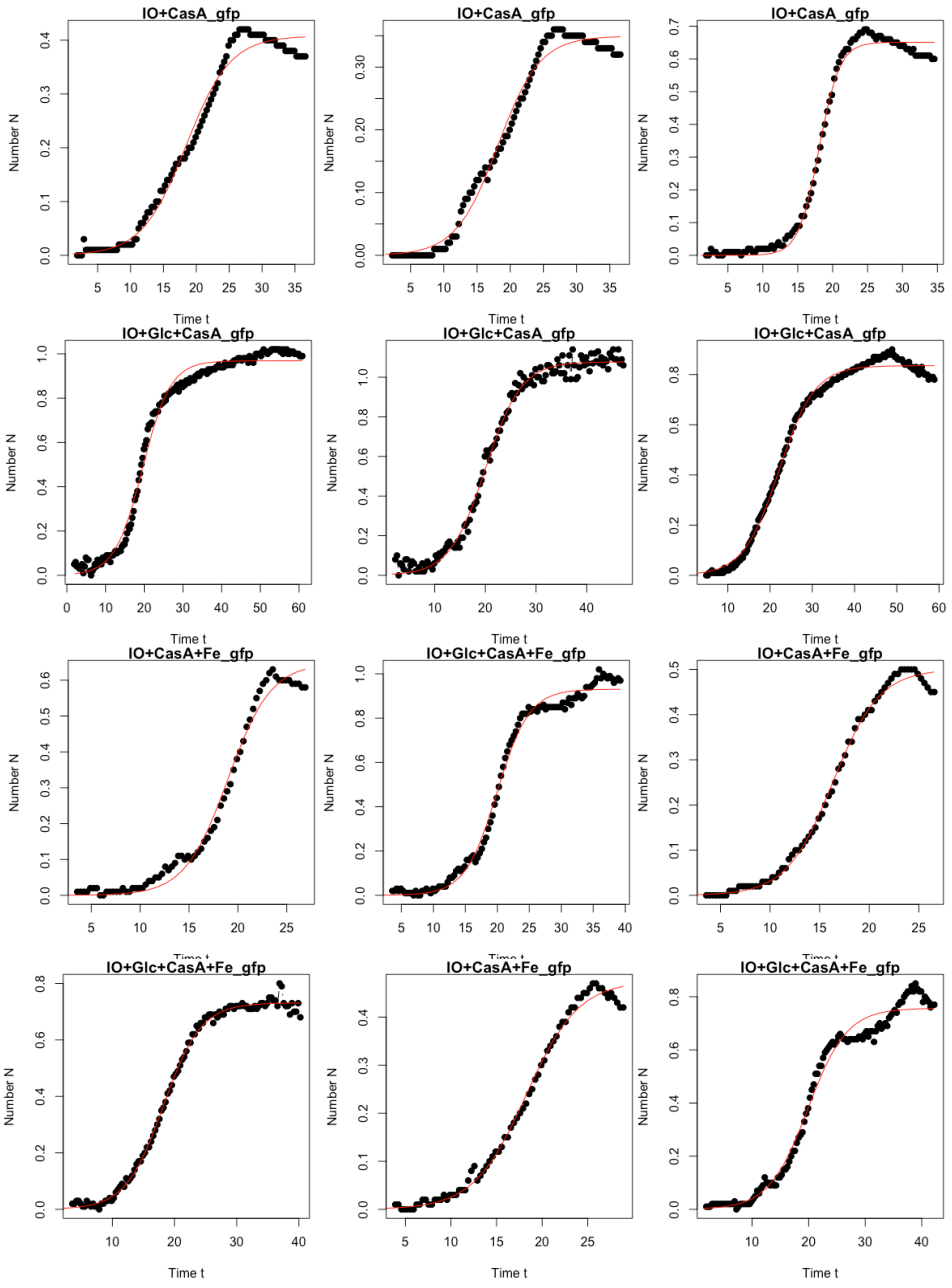

Appendix 2. OD600 Growth Data modelled to fit logistic regression to extract the functional parameters such as carrying capacity, growth rate and generation time. Models are shown for *P. piscinae*-GFP strain grown on the following media compositions: IO+CasA, IO+Glc+CasA, IO+CasA+Fe & IO+Glc+CasA+Fe

Bibliography

[1] - Nations, U., of Economic, D., Affairs, S., & Division, P. (n.d.). *World Population Prospects 2022 World Population Prospects 2022 Summary of Results*.

[2] - The State of World Fisheries and Aquaculture 2022. In *The State of World Fisheries and Aquaculture 2022*. Food and Agriculture Organization of the United States

[3] - Cabello, F. C., Godfrey, H. P., Tomova, A., Ivanova, L., Dölz, H., Millanao, A., & Buschmann, A. H. (2013). Antimicrobial use in aquaculture re-examined: Its relevance to antimicrobial resistance and to animal and human health. *Environmental Microbiology*, *15*(7), 1917–1942. https://doi.org/10.1111/1462-2920.12134

[4] - Bentzon-Tilia, M., Sonnenschein, E. C., & Gram, L. (2016). Monitoring and managing microbes in aquaculture – Towards a sustainable industry. *Microbial Biotechnology*, *9*(5), 576–584. https://doi.org/10.1111/1751-7915.12392

[5] - Grotkjær, T., Bentzon-Tilia, M., D'Alvise, P., Dourala, N., Nielsen, K. F., & Gram, L. (2016). Isolation of TDA-producing Phaeobacter strains from sea bass larval rearing units and their probiotic effect against pathogenic Vibrio spp. in Artemia cultures. *Systematic and Applied Microbiology*, *39*(3), 180–188. https://doi.org/10.1016/j.syapm.2016.01.005

[6] - Grotkjær, T., Bentzon-Tilia, M., D'Alvise, P., Dierckens, K., Bossier, P., & Gram, L. (2016). Phaeobacter inhibens as probiotic bacteria in non-axenic Artemia and algae cultures. *Aquaculture*, *462*, 64–69. https://doi.org/10.1016/j.aquaculture.2016.05.001

[7] - Gram, L., Rasmussen, B. B., Wemheuer, B., Bernbom, N., Ng, Y. Y., Porsby, C. H., Breider, S., & Brinkhoff, T. (2015). Phaeobacter inhibens from the Roseobacter clade has an environmental niche as a surface colonizer in harbors. *Systematic and Applied Microbiology*, *38*(7), 483–493. https://doi.org/10.1016/j.syapm.2015.07.006

[8] - Wilson, M. Z., Wang, R., Gitai, Z., & Seyedsayamdost, M. R. (2016). Mode of action and resistance studies unveil new roles for tropodithietic acid as an anticancer agent and the glutamyl cycle as a proton sink. *Proceedings of the National Academy of Sciences of the United States of America*,

113(6), 1630–1635. https://doi.org/10.1073/pnas.1518034113

[9] - Beyersmann, P. G., Tomasch, J., Son, K., Stocker, R., Göker, M., Wagner-Döbler, I., Simon, M., & Brinkhoff, T. (2017). Dual function of tropodithietic acid as antibiotic and signaling molecule in global gene regulation of the probiotic bacterium Phaeobacter inhibens. *Scientific Reports*, *7*(1). https://doi.org/10.1038/s41598-017-00784-7

[10] - Geng, H., Bruhn, J. B., Nielsen, K. F., Gram, L., & Belas, R. (2008). Genetic dissection of tropodithietic acid biosynthesis by marine roseobacters. *Applied and Environmental Microbiology*, *74*(5), 1535–1545. https://doi.org/10.1128/AEM.02339-07

[11] - D'Alvise, P. W., Phippen, C. B. W., Nielsen, K. F., & Gram, L. (2016). Influence of iron on production of the antibacterial compound tropodithietic acid and its noninhibitory analog in Phaeobacter inhibens. *Applied and Environmental Microbiology*, *82*(2), 502–509. https://doi.org/10.1128/AEM.02992-15

[12] - Duan, Y., Petzold, M., Saleem-Batcha, R., & Teufel, R. (2020). Bacterial Tropone Natural Products and Derivatives: Overview of their Biosynthesis, Bioactivities, Ecological Role and Biotechnological Potential. In *ChemBioChem* (Vol. 21, Issue 17, pp. 2384–2407). Wiley-VCH Verlag. https://doi.org/10.1002/cbic.201900786

[13] - Geng, H., Bruhn, J. B., Nielsen, K. F., Gram, L., & Belas, R. (2008). Genetic dissection of tropodithietic acid biosynthesis by marine roseobacters. *Applied and Environmental Microbiology*, *74*(5), 1535–1545. https://doi.org/10.1128/AEM.02339-07

[14] - Jaishankar, J., & Srivastava, P. (2017). Molecular basis of stationary phase survival and applications. In *Frontiers in Microbiology* (Vol. 8, Issue OCT). Frontiers Media S.A. https://doi.org/10.3389/fmicb.2017.02000

[15] - Li, X., Zhao, X., Fang, Y., Jiang, X., Duong, T., Fan, C., Huang, C.-C., & Kain, S. R. (1998). *Generation of Destabilized Green Fluorescent Protein as a Transcription Reporter**. http://www.jbc.org

[16] - Brock, N. L., Nikolay, A., & Dickschat, J. S. (2014). Biosynthesis of the antibiotic tropodithietic acid by the marine bacterium Phaeobacter inhibens. *Chemical Communications*, *50*(41), 5487–5489. https://doi.org/10.1039/c4cc01924e

[17] - D'Alvise, P. W., Magdenoska, O., Melchiorsen, J., Nielsen, K. F., & Gram, L. (2014). Biofilm formation and antibiotic production in Ruegeria mobilis are influenced by intracellular concentrations of cyclic dimeric guanosinmonophosphate. *Environmental Microbiology*, *16*(5), 1252–1266. https://doi.org/10.1111/1462-2920.12265

[18] - Geng, H., & Belas, R. (2010). Expression of tropodithietic acid biosynthesis is controlled by a novel autoinducer. *Journal of Bacteriology*, *192*(17), 4377–4387. https://doi.org/10.1128/JB.00410-10

[19] - Vallenet, D., Calteau, A., Dubois, M., Amours, P., Bazin, A., Beuvin, M., Burlot, L., Bussell, X., Fouteau, S., Gautreau, G., Lajus, A., Langlois, J., Planel, R., Roche, D., Rollin, J., Rouy, Z., Sabatet, V., & Médigue, C. (2020). MicroScope: An integrated platform for the annotation and exploration of microbial gene functions through genomic, pangenomic and metabolic comparative analysis. *Nucleic Acids Research*, *48*(D1), D579–D589. https://doi.org/10.1093/nar/gkz926

[20] - Weiten, A., Kalvelage, K., Neumann-Schaal, M., Buschen, R., Scheve, S., Winklhofer, M., & Rabus, R. (2022). Nanomolar Responsiveness of Marine Phaeobacter inhibens DSM 17395 toward Carbohydrates and Amino Acids. *Microbial Physiology*, *32*(3–4), 108–121. https://doi.org/10.1159/000524702

[21] - Neilands, J. B. (1995). *Siderophores: Structure and Function of Microbial Iron Transport Compounds**.

[22] - Braun, V., & Hantke, K. (2011). Recent insights into iron import by bacteria. In *Current Opinion in Chemical Biology* (Vol. 15, Issue 2, pp. 328–334). https://doi.org/10.1016/j.cbpa.2011.01.005

[23] - Mridha, S., & Kümmerli, R. (2022). Coordination of siderophore gene expression among clonal cells of the bacterium Pseudomonas aeruginosa. *Communications Biology*, *5*(1). https://doi.org/10.1038/s42003-022-03493-8

[24] - Sonnenschein, E. C., Phippen, C. B. W., Nielsen, K. F., Mateiu, R. V., Melchiorsen, J., Gram, L., Overmann, J., & Freese, H. M. (2017). Phaeobacter piscinae sp. nov., a species of the Roseobacter group and potential aquaculture probiont. *International Journal of Systematic and Evolutionary Microbiology*, *67*(11), 4559–4564. https://doi.org/10.1099/ijsem.0.002331

[25] - Tackling drug-resistant infections globally: final report and recommendations the review on antimicrobial resistance chaired by Jim O'Neill. (2016).

[26] - Rabe, P., Klapschinski, T. A., Brock, N. L., Citron, C. A., D'Alvise, P., Gram, L., & Dickschat, J. S. (2014). Synthesis and bioactivity of analogues of the marine antibiotic tropodithietic acid. *Beilstein Journal of Organic Chemistry*, *10*, 1796–1801. https://doi.org/10.3762/bjoc.10.188

[27] - Prol García, M. J., D'Alvise, P. W., Rygaard, A. M., & Gram, L. (2014). Biofilm formation is not a prerequisite for production of the antibacterial compound tropodithietic acid in Phaeobacter inhibens DSM17395. *Journal of Applied Microbiology*, *117*(6), 1592–1600. https://doi.org/10.1111/jam.12659

[28] - Sprouffske, K., & Wagner, A. (2016). Growthcurver: An R package for obtaining interpretable metrics from microbial growth curves. *BMC Bioinformatics*, *17*(1). https://doi.org/10.1186/s12859-016-1016-7

[29] - Ringø, E., Olsen, R. E., Jensen, I., Romero, J., & Lauzon, H. L. (2014). Application of vaccines and dietary supplements in aquaculture: possibilities and challenges. Reviews in Fish Biology and Fisheries, 24(4), 1005–1032. https://doi.org/10.1007/s11160-014-9361-y

[30] - Resistance, A. (2021). Norm Norm - Vet 2021. 2307.

[31] – Martin, J.H. & Fitzwater, S.E. (1988). Iron deficiency limits phytoplankton growth in the north-east Pacific subarctic. Nature, 331, 341-343.

[32] - Gonza´lez, J. M., Gonza´lez, G., Whitman, W. B., Hodson, R. E., & Moran, M. A. (1996). Identifying Numerically Abundant Culturable Bacteria from Complex Communities: an Example from a Lignin Enrichment Culture. In *APPLIED AND ENVIRONMENTAL MICROBIOLOGY* (Vol. 62, Issue 12).

[32] - F/2, Guillard, R.R.L. 1975. Culture of phytoplankton for feeding marine invertebrates. pp 26-60. Smith W.L. and Chanley M.H (Eds.) Culture of Marine Invertebrate Animals. Plenum Press, New York, USA